





## Article

# Assessment of the Effect of Corona Discharge on Synchronous Generator Self-Excitation

Huthaifa A. Al\_Issa <sup>1</sup>, Marcin Drechny <sup>2,\*</sup>, Issam Trrad <sup>3</sup>, Mohamed Qawaqzeh <sup>1</sup>, Vladislav Kuchanskyy <sup>4,\*</sup>, Olena Rubanenko <sup>5,6,\*</sup>, Stepan Kudria <sup>6</sup>, Petro Vasko <sup>7</sup>, Oleksandr Miroshnyk <sup>8</sup> and Taras Shchur <sup>9</sup>

- <sup>1</sup> Department of Electrical and Electronics Engineering, Al Balqa Applied University, Al Salt 19117, Jordan; h.alissa@bau.edu.jo (H.A.A.); qawaqzeh@bau.edu.jo (M.Q.)
  - <sup>2</sup> Institute of Electrical Engineering, Faculty of Telecommunications, Computer Science and Electrical Engineering, Bydgoszcz University of Science and Technology, 85-796 Bydgoszcz, Poland
  - <sup>3</sup> Department of Communication and Computer Engineering, Jadara University, Irbid 21110, Jordan; itradd@jadra.edu.jo
  - <sup>4</sup> Institute of Electrodynamics of NAS of Ukraine, Str. Peremohy, 56, 03057 Kyiv, Ukraine
  - <sup>5</sup> Department of Electrical Stations and Systems, Vinnytsia National Technical University, Khmelnytsky Highway, 95, 21021 Vinnytsya, Ukraine
  - <sup>6</sup> Department of Wind Power, Institute of Renewable Energy of the National Academy of Sciences of Ukraine, St. Hnata Khotkevycha 20-a, 02094 Kyiv, Ukraine; sa.kudria@gmail.com
  - <sup>7</sup> Department of Hydropower, Institute of Renewable Energy of the National Academy of Sciences of Ukraine, St. Hnata Khotkevycha 20-a, 02094 Kyiv, Ukraine; ivevasko@gmail.com
  - <sup>8</sup> Department of Electricity and Energy Management, State Biotechnological University, Str. Rizdviana, 19, 61052 Kharkiv, Ukraine; omiroshnyk@ukr.net
  - <sup>9</sup> Department of Cars and Tractors, Faculty of Mechanics and Energy, Lviv National Agrarian University, Str. Volodymyr Great, 1, 80381 Dubliany, Ukraine; shchurtg@gmail.com
- \* Correspondence: marcin.drechny@pbs.edu.pl (M.D.); kuchanskiyvladislav@gmail.com (V.K.); olenarubanenko@ukr.net (O.R.); Tel.: +380-503-878-942 (V.K.); +380-977-480-285 (O.R.)



**Citation:** Al\_Issa, H.A.; Drechny, M.; Trrad, I.; Qawaqzeh, M.; Kuchanskyy, V.; Rubanenko, O.; Kudria, S.; Vasko, P.; Miroshnyk, O.; Shchur, T. Assessment of the Effect of Corona Discharge on Synchronous Generator Self-Excitation. *Energies* **2022**, *15*, 2024. <https://doi.org/10.3390/en15062024>

Academic Editor: Ferdinanda Ponci

Received: 26 January 2022

Accepted: 8 March 2022

Published: 10 March 2022

**Publisher's Note:** MDPI stays neutral with regard to jurisdictional claims in published maps and institutional affiliations.



**Copyright:** © 2022 by the authors. Licensee MDPI, Basel, Switzerland. This article is an open access article distributed under the terms and conditions of the Creative Commons Attribution (CC BY) license (<https://creativecommons.org/licenses/by/4.0/>).

**Abstract:** The method of operative determination of active power losses (both loading and crown) in alternating current lines has been improved. The proposed technique allows monitoring of active power losses in lines. Based on the comparative analysis of different approximation methods, the most effective method of analytical representation of regression dependences of active power losses on the corona on voltage for different weather conditions is proposed. The validity and reliability of scientific statements, conclusions, and recommendations given in the dissertation are confirmed by the analysis of the results of comparative calculations performed for different models. The efficiency of the developed algorithms and programs was tested on control examples with reference source data, where the results of the calculations were compared with the results obtained by standard programs. The developed technique of operative determination of losses of active power (loading and on a crown) allows one to carry out current monitoring of losses and passive parameters of high-voltage power lines of alternating current. The phenomena of self-excitation of generators connected to unloaded power lines are considered at great length. A physical analysis of the ongoing processes is given, and calculation methods are proposed that have been experimentally tested on a dynamic model. The paper takes into account the effect of the wire corona on the conditions of self-excitation of generators with the necessary developments to prevent this negative phenomenon in the main electrical network. Models and methods have been developed for evaluating the effect of the wire corona on the conditions for the occurrence of self-excitation in ultra-high voltage transmission lines.

**Keywords:** controlled shunt reactor; corona discharge power losses; flexible alternating current transmission systems; self-exciting synchronous generator; STATCOM

## 1. Introduction

There are many works that consider the problem of self-excitation of generators in main electrical networks when generators of power plants operate on an unloaded line [1–4].

Briefly, the process of self-excitation of the generator, with negative consequences for the operation of the electrical network, can be described as follows.

In the unloaded mode of operation of the ultra-high voltage transmission line (UHV), there is an issue not only with the auto-parametric self-excitation of paired harmonic components with a resonant voltage increase but also the self-excitation of generators. In this mode, the charging power of the line can significantly exceed the rated power of the generators connected to the power transmission line [5,6]. This leads to the self-excitation of generators, and their terminals have an existing voltage that does not match the excitation current. That is, the possibility of self-excitation and its nature largely depends on the ratio between the rated power of the power plants generators and the charging power of the line. The degree of compensation of the charging capacity of the line during the design is calculated at 60–80% according to the available capacity of shunt reactors, which are manufactured in factories [7,8]. Providing the necessary degree of charge power compensation for a specific solution to the operational problem is problematic due to the inability to regulate the inductance of the shunt reactor. In this case, the issue of regulated compensation of charging power is acute to prevent the occurrence of negative phenomena, including the self-excitation of generators.

Moreover, the works do not indicate why it is necessary to prevent the self-excitation of generators, because it is not always possible to install high-speed regulators on synchronous generators to remove them from the self-excitation regions. Furthermore, in such works, the fact is stated that one of the key reasons for the occurrence of self-excitation is excess charging power without the subsequent development of measures to prevent self-excitation. It was found [8–10] that the excess reactive power of the line is one of the main causes of self-excitation, therefore by regulating the reactive power flow with adjustable reactive power devices, these values can be reduced to the required level.

It should be noted that the work did not take into account the effect of corona wires on the process of self-excitation of the generator [10–12]. First of all, the papers did not consider how exactly it is necessary to take into account the corona discharge, due to the fact that mathematical methods for estimating the effect of active power losses on the corona discharge are not presented. In robots, corona losses are taken into account by approximate engineering methods and models of the physical process of the occurrence and existence of a corona discharge [13]. Taking into account the fact that active conductivity and capacitance between the phase and ground increase during the corona wire, there is a need to evaluate the change in the values of equivalent conductivities of the equivalent circuit of an overhead power transmission line.

## 2. Establishment Processes in Non-Saturated Machine

Based on the proposed method of taking into account the magnetic characteristics of the machine in the differential equations of electromagnetic processes, an existing theory is added, termed asynchronous self-excitation, a preliminary analysis of which was given in [5–7].

Recall that in the theory we are developing, self-excitation of an oscillatory system formed by a synchronous machine and a capacitive load is understood as the generation of continuous free oscillations under the influence of periodic changes in the parameters of the system in the absence of any external e.m.f. from external sources of excitation (direct current excitation, residual field). The origin of free oscillations occurs as a result of some initial perturbations of the state of the rest of the system (the e.m.f. and the current in the circuits of the system are equal to zero). The ideal curve of magnetization of the machine is taken (hysteretic with a linear initial section  $m_0$  (Figure 1)), therefore if the conditions of self-excitation in this section are met, the initial disturbances can be arbitrarily small [14,15]. In reality, for the occurrence of increasing oscillations and the presence of residual emulsion, idling of the order of several volts as an initial disturbance is required.

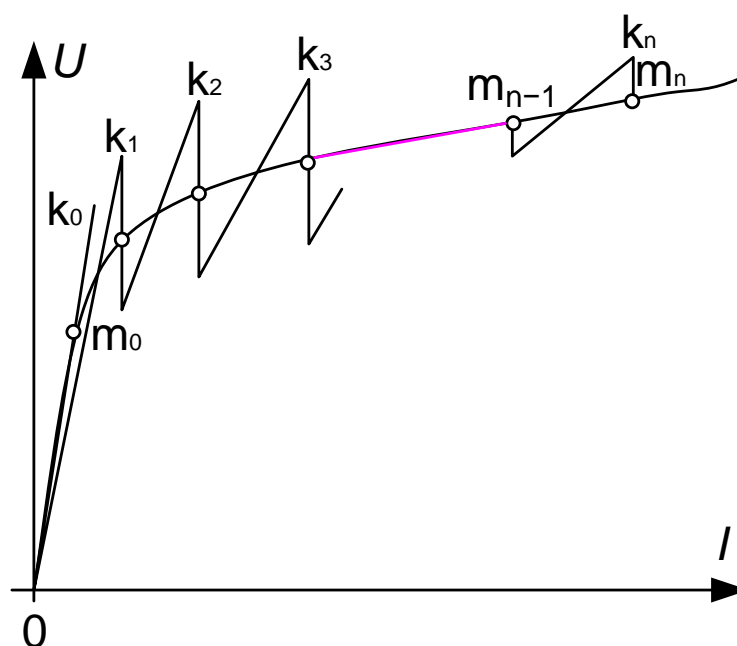


Figure 1. Replacing the magnetization curve with a stepped characteristic.

The charging power of the line can significantly exceed the rated power of the generators connected to the power line, which leads to their unacceptable overload. Generators connected to an unloaded power line can self-excite. Self-excitation is understood as a mode of operation of generators in which a certain voltage is spontaneously established at their terminals and on the line, which does not correspond to the excitation current of the generators. The station maintenance personnel lose the ability to control the established voltage, the value of which at individual transmission points can significantly exceed the permissible values. The possibility of self-excitation and its nature depends on the ratio between the nominal power of the power plant generators and the charging power of the transmission line. The voltage at the open end of the unloaded line with incomplete compensation of its charging power significantly exceeds the voltage at the beginning of the power transmission. Therefore, in order to synchronize the remote station and the receiving system using conventional methods, it is necessary to lower the voltage at the beginning of the transmission or install compensating devices at its end. Reducing the voltage at the beginning of long-distance power transmission can be difficult due to the possibility of self-excitation of the generators of the remote station.

The study of electromagnetic phenomena in rotating machines can be approached from two mutually complementary points of view, reflecting different aspects of the general physical process: (1) To study oscillatory processes directly in the contours of the machine; (2) to investigate the behavior of the resulting electromagnetic field of the machine, created by all contour flux linkages, voltages, and currents in the aggregate.

In an unsaturated three-phase synchronous machine with uniaxial winding on the rotor (we do not take into account hidden circuits), in the first method, the initial method comprises linear differential equations compiled with respect to variables  $a$ ,  $b$ ,  $c$ , and  $d$ , either in phase coordinates  $\alpha$ ,  $\beta$ ,  $\gamma$  or in coordinates as was applied in Equations (1)–(5).

In any mode of operation of a synchronous machine, differential equations of oscillations in circuits will contain periodic coefficients due to periodic changes in the stator inductances (when  $x_d \neq x_q$  and  $x'_d \neq x'_q$ ) and the mutual inductance between the stator and the rotor.

For a symmetrical load, we obtain the equations with constant coefficients:

$$\begin{cases} x_d' \frac{di_d}{d\theta} = -ri_d - x_q i_q + \rho_0 u_r - e_d \\ x_q \frac{di_q}{d\theta} = -ri_q + x_d i_d + u_r - e_q \\ \frac{du_r}{d\theta} = -\rho_1 u_r + \chi(r i_d + x_q i_q + e_d) \\ \frac{du_c}{d\theta} = -e_q + x_c i_d \\ \frac{du_r}{d\theta} = e_d + x_c i_q \end{cases} \quad (1)$$

The characteristic equation of system (1) is written in the following form:

$$D(p) = \begin{vmatrix} -(p + \frac{r}{x_d}) & -\frac{x_q}{x_d} & \frac{\rho_0}{x_d'} & -\frac{1}{x_d'} & 0 \\ \frac{x_d}{x_q} & -(p + \frac{r}{x_q}) & \frac{1}{x_q} & 0 & -\frac{1}{x_q} \\ xr & \chi x_q & -(p + \rho_1) & \chi & 0 \\ x_c & 0 & 0 & -p & -1 \\ 0 & x_c & 0 & 1 & -p \end{vmatrix} \quad (2)$$

In an expanded form, instead of (2), we have:

$$D(p) = a_0 p^5 + a_1 p^4 + a_2 p^3 + a_3 p^2 + a_4 p + a_5 = 0 \quad (3)$$

where

$$a_0 = x_d' x_q \quad (4)$$

$$a_1 = x_d x_q \rho_0 + (x_d' + x_q) r \quad (5)$$

$$a_2 = 2x_d' x_q + x_c (x_d' + x_q) + r \rho_0 (x_d + x_q) + r^2 \quad (6)$$

$$a_3 = (2x_d' x_q + x_c (x_d' + x_q)) \rho_0 + (2x_c + x_d' + x_q) r + r^2 \rho_0 \quad (7)$$

$$a_4 = (x_c - x_d') (x_c - x_q) + (2x_c + x_d + x_q) r \rho_0 + r^2 \quad (8)$$

$$a_5 = ((x_c - x_q) (x_c - x_d) + r^2) \rho_0 \quad (9)$$

Equation (1) comprises the equations of the components of the envelope amplitudes of phase oscillations of the stator: The sweep of the hodographs of generalized vectors  $\dot{e} = e_d \pm j e_q$  and  $i = i_d \pm j i_q$  gives the envelopes of vibrations stator at a certain scale. This property of the equations in coordinates  $d, q$  remains in force even in the presence of modulating terms due to the asymmetry of the load.

### 3. Establishment Processes in a Saturated Machine

Instead of unbounded fluctuations obtained by the self-excitation of unsaturated machines, in the case of a saturated machine, free vibrations in the circuits and the resulting electromagnetic field only increase up to some finite amplitude determined by the degree of saturation. As one increases the amplitude, the magnetization machine build-up speed gradually decreases, reaching zero at stationary modes of self-excitation. Mathematically, the establishment process should be nonlinear differential equations, covering the entire process of establishment in general, the solutions of which should reflect the specified gradual decrease in speed and increase in amplitude. However, due to the lack of any general methods for integrating nonlinear differential equations, it is necessary to search for such approximate methods that, to some extent, reflect the physical picture of the processes under consideration [15–18].

As a first approximation, consider the method of taking into account the magnetic characteristics of the machine at discrete intervals. Let us break the magnetization curve into separate intervals, from 0 to  $m_0$ , from  $m_0$  to  $m_1$ , from  $m_1$  to  $m_2$ , etc. (Figure 1), ending with the interval from  $m_{n-1}$  to  $m_0$ . Let us say that the processes of interest to us are running within the interval  $m_0 m_1$ . If in this interval the curve is replaced by a ray segment, then the inductance machines defined by its slope will be less than the values  $0m_0$  in the section

from 0. Substituting these “saturated” values in (1), we obtain the first approximation to the true unsteady processes on the interval  $m_0m_1$  of the curve magnetization. Accordingly, the real part of  $p_{1,2}$  roots with asynchronous self-excitation is decreased.

In the next interval  $m_1m_2$ , the ray  $OK_2$  will determine even smaller inductances and, accordingly, the increment will decrease even more. Continuing this process, we will finally reach the interval  $m_{n-1}m_n$ , where the growth increment vanishes, and it will be the one range of magnetic characteristics, within which we will establish a stationary regime of the given type of self-excitation. Within each interval, the amplitude of oscillations increases along with the exponential function  $e^{v\theta}$ , but the envelope of all partial exponentials certainly approaches the true settling curve at a continuously decreasing build-up speed.

Establishment processes that can be visualized are also depicted as follows.

On the plane  $r, x_c$ , where  $r$  is the active resistance of phase stator windings and  $x_c$  is the capacitive load resistance, let us select self-excitation zones for unsaturated three-phase salient machines (Figure 2). For synchronous self-excitation, this will be the area  $a_5 < 0$  bounded by a parabola  $a_5 = 0$  and the area  $\Delta_4 < 0$ , with a limited curve  $\Delta_4 = 0$ , where

$$\Delta_4 = \begin{vmatrix} a_1 & a_0 & 0 & 0 \\ a_3 & a_2 & a_1 & a_0 \\ a_5 & a_4 & a_3 & a_2 \\ 0 & 0 & a_5 & a_4 \end{vmatrix} = 0$$

is the penultimate Hurwitz determinant for the characteristic Equation (3). In practical cases, equality  $\Delta_4 = 0$  can be replaced by equality  $a_4 = 0$ . On the boundary  $a_4 = 0$ , Equation (2) has a pair of purely imaginary roots  $p_{1,2} = \pm j$ .

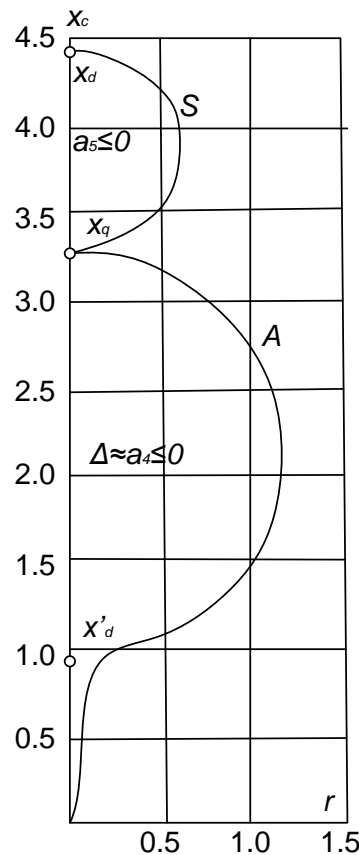


**Figure 2.** Partition of the plane  $r, x_c$  into zones of instability (three-phase, salient pole generator,  $x'_d = 0.95, x_q = 3.29, x_d = 4.46, \rho \approx 10^{-3}$ ). S is the border of synchronous self-excitation; A is the border of asynchronous self-excitation.

Let the parameters of the given system machine load correspond to the point  $A$  on the plane  $r, x_c$  (Figure 3), and  $A^{(0)}$  is the boundary of asynchronous self-excitation at unsaturated values of inductance machines on the interval  $Om_0$  of the magnetization curve. In this case, the characteristic Equation (2) admits complex  $p_{1,2}^{(0)} = \vartheta^{(0)} \pm j_0^{(0)}$ , where  $\vartheta^{(0)} > 0$ . When the machine goes to the interval  $m_0m_1$ , then the boundary of the asynchronous self-excitation will serve as a curve  $A^{(1)}$ , limiting the region of instability, at the point  $M$  of which  $\vartheta^{(1)} < \vartheta^{(0)}$ . It is obvious that an increase in the amplitude of the variables  $i_d, i_q, u_r, e_d, e_q$  will continue until after the point  $M$  does not pass the boundary  $A^{(n)}$ , with the corresponding interval  $m_{n-1}m_n$ . Since, on this border  $p_{1,2}^{(0)} = \pm j_0^{(0)}$ , that is, the growth rate  $\vartheta^{(n)} = 0$ , the amplitude of oscillations in the contours, and the resulting electromagnetic field of the machine increased further.

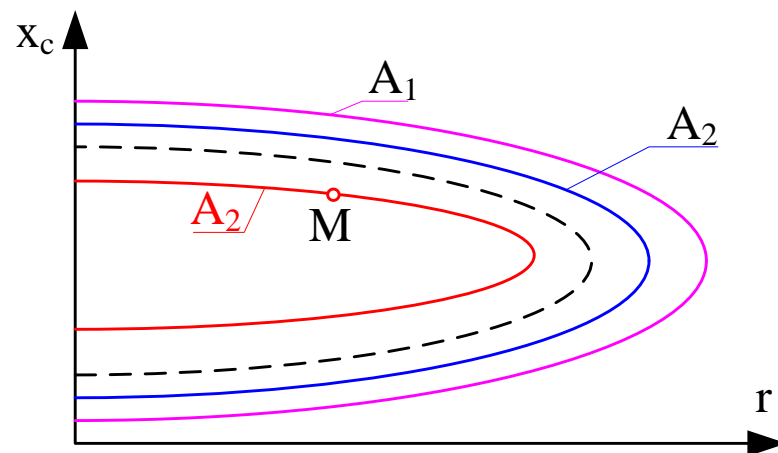


**Figure 3.** Asynchronous border movement self-excitation in the process establishment.

From the fact that negative values of the determinant  $\Delta_4$  and coefficient  $a_4$  at the point  $M$  are caused by the inequalities  $x_d' < x_c < x_q$ , it follows that the tendency of  $\Delta_4$  and  $a_4$  to move towards zero when moving boundaries of asynchronous self-excitation to  $M$  is determined primarily by the saturation of the machine in the transverse axis and, consequently, a decrease in the difference of  $x_c - x_q$  [1].

A similar picture can be drawn for synchronous self-excitation by replacing the curve  $A^{(m)}$  with the curve  $S^{(m)}$  on  $a_5^{(m)} = 0$ . In this case,  $a_5 = 0$  is concerned primarily with saturation in the longitudinal axis and a decrease in the difference  $x_c - x_q$  ( $a_5 \leq 0$  due to conditions  $x_q < x_c < x_d$ ); slew rate fluctuations decrease to zero due to the gradual decrease to zero positive of the real root of Equation (2):

$$p_5^{(0)} > p_5^{(1)} > p_5^{(2)} > \dots > p_5^{(n)} = 0 \quad (10)$$

#### 4. Development of Measures to Prevent Self-Excitation of Generators

If the power transmitted through the EHV (extra high voltage) line is less than the natural one, and the length of the power transmission is less than a half-wave, then there will be an excess of reactive power in the line and its flows will be directed from the line [13–16]. This can lead to increased voltage levels that can exceed the highest operating and short-term allowable values. Increased voltage levels adversely affect the operation of electrical equipment, causing it to age faster, and can also lead to failure. Therefore, in low-load modes, it is necessary to limit the flow of reactive power from the line. For this, as a rule, shunt reactors are used; however, as noted earlier, their efficiency decreases in terms of increasing the throughput and compensating for reactive power in a wide range of operating modes. This problem can be effectively solved using controlled shunt reactors. Their required power is determined by the nominal line voltage, its total length, and the length of the sections between intermediate substations, the transmitted active power, the

operating conditions of the transmitting station generators, and the characteristics of the receiving system, as well as the need to maintain the line voltage within reasonable limits.

The analytical expressions for the coefficients of the characteristic polynomial obtained after the expansion in the power of the operator “ $p$ ” of the determinant of the system of equations of small perturbations (with neglect of transient processes in stator circuits) in the absence of excitation regulation and neglect of the damper circuits of the generators have the form:

$$a_0 = \frac{T_j T_{d0}}{\omega_0} B_q B'_d \quad (11)$$

$$a_1 = \frac{T_j}{\omega_0} B_q B_d \quad (12)$$

$$a_2 = T_{d0} \left[ B_q B'_d S_E + (x_d - x'_d) \left( 2 - \frac{B_d}{B_q} \right) U_2^2 \sin^2 \delta_0 \right] \quad (13)$$

$$a_3 = B_q B_d S_E \quad (14)$$

where  $S_E = \frac{B_q U_2^2}{B_d} \cos \delta_0 + \frac{U_2^2}{D} \left( \frac{1}{B_q} - \frac{1}{B_d} \right) \cos 2\delta_0$  is the power transmission,  $B_d = B + D(x_d + x_{T1})$ ,  $B_q = B + D(x_q + x_{T1})$  is the total resistance of the power transmission in the longitudinal and transverse axes;  $B'_d = B + D(x'_d + x_{T1})$  is the total transient resistance of the power transmission,  $B$ ,  $D$  are equivalent generalized line parameters, and  $\delta$  is the total angle of transmission. In the entire considered range of line and under any operating modes  $\cos \delta_0 < 0$ , it is easy to establish that with the adopted idealization of the system, all the coefficients of the characteristic polynomial can be positive only in the IV zone. The second zone of the range under consideration is a zone of scrambled self-excitation, the third is a zone of repulsion–synchronous self-excitation, and the fourth is a zone of asynchronous self-excitation. The self-excitation zones of a hydrogenerator with typical parameters, with built-in coordinates [I, R), are shown in Figure 4.

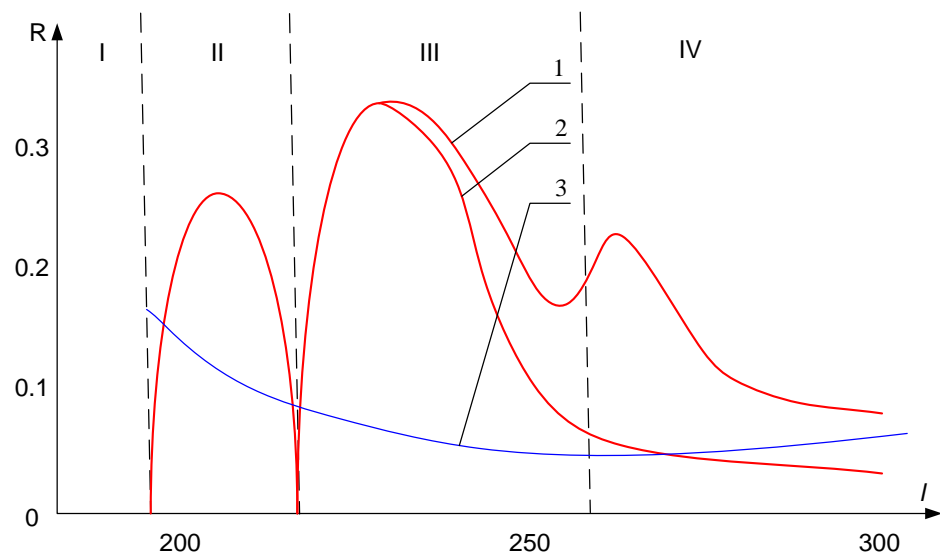


**Figure 4.** Generator self-excitation zones (the installed power of the transmitting station is equal to the natural power of the line).

### 5. Regulation of EHV Network Modes by Voltage Taking into Account Corona Losses

The regulation of the power factors on the buses of terminal substations can be carried out by changing the excitation currents of the windings of the rotors of the synchronous generators of power plants and synchronous compensators located in the interconnected power systems near or directly at the terminal substations of the power transmission. This

control affects both the improvement of the quality of the electrical energy supplied to the receiving system and the voltage mode directly in the line itself.

Changing the composition of power transmission equipment during its operation is carried out by turning on (turning off) shunt reactors and other transverse compensation devices located at the intermediate PP of the line, as well as transverse compensation devices installed at its terminal substations. Such an impact will lead to a direct change in the reactive power regime in the power transmission and at its terminal substations, an indirect positive effect on the voltage regime along the line route, and, as a consequence, an improvement in the quality of electrical energy in the receiving system.

Energy losses in the power plant are directly proportional to the established standards and electricity tariffs, so measures to reduce them are always an urgent task. To solve the problem of minimizing energy losses, it is very important to classify each component of all possible losses without exception. However, not all energy losses are normalized, and their accounting is carried out according to indications of electricity supply to the grid and consumers, adjusted for load factors, which worsens the accuracy of the calculation. Additionally, some types of loss are not mentioned at all as an ongoing physical process. This raises the problem of studying and substantiating non-normalized losses.

In the physical essence, the corona represents a stable electrical discharge in sharply inhomogeneous fields, where the emerging streamers cannot completely cover the space between the electrodes, and ionization is a limited area near the potential electrode with a small radius of curvature (case crowns). On the overhead line, the crown can be observed in two manifestations: In the form of a crown series and surface partial discharges. Corona discharge by all characteristics and manifestations is a low-current discharge, which does not reduce the voltage across the discharge gap and can glow for hours and days. With an increase in the field strength at the electrode, the initial corona in the form of a halo "diverges" into separate foci, in which, in fractions of a microsecond, ever longer luminous formations continuously arise, wherein thin channels are sources of cold light streamers. When exposed to impulse voltages of the megavolt range, the length of the streamers can reach several  $k_i$  meters. The streamer corona does not lead to a short circuit, and for this, it is necessary, at a minimum, that the streamer channels cross the entire gap, which occurs at an average field strength in atmospheric air of 5 kV/cm.

The efficiency of operational optimization of electric power system (EPS) modes in terms of voltage and reactive power will increase when using real, or close to real, quickly determined dependences of active power losses to the corona on the nodal voltages at the ends of high-voltage lines ( $\Delta P_k = f(U)$ ) in the calculations. In turn, the on-line determination of the dependences  $\Delta P_k = f(U)$  presupposes the solution of problems on the choice of a method for their approximation and an approach to the correct estimation of the optimal degree of the approximating polynomial. The results of solving these problems are given in the fourth section of this thesis. Three methods of the approximation of regression dependences  $\Delta P_k = f(U)$  were investigated: Polynomial regression, sequential regression, and orthogonal Chebyshev polynomials. The study of approximation methods was carried out using materials available in bulk electrical power systems (curves of the dependence of specific corona losses on voltage), obtained by corresponding measurements on a 750 kV power transmission line for four types of weather.

The results of calculating the dependences  $\Delta P_k = f(U)$  for mixed types of weather conditions are presented. A comparative analysis of these approximation methods is carried out to solve the problem of promptly determining the dependences of corona power losses on voltage for various weather conditions. A statistically correct estimate of the choice of the required degree of the approximating polynomial is proposed.

## 6. Structural and Parametric Identification of the Dependences of Active Power Losses on the Corona on Voltage

When solving problems of the operational control of EPS, after assessing the state, for example, using software complexes [16–18], as a rule, operational optimization of the



current mode in terms of voltage and reactive power is carried out. At the same time, in the existing optimization programs, to take into account the power losses for the corona, the recommendations given in [19–21] are followed and the typical dependences of the power losses for the corona on the voltage levels ( $\Delta P_k = f(U)$ ) for various brands of wires and certain typical weather conditions are obtained. The “Guidelines for Accounting for Corona Losses and Corona Interference” identifies four main groups of weather types, each with a different average corona loss: The first group is good weather; the second is dry snow; the third is rain; the fourth is frost. The duration of the influence of weather conditions of individual groups on the duration of the existence of the corona and its characteristics may decrease under the influence of heating the wires by the load current. At current densities higher than some values, called critical, atmospheric deposits in the form of frost, dew, crystalline frost, or the smallest droplets of water (fog, high humidity, low-intensity rain) are not formed on the surface of the wires. As a consequence, corona losses under specified meteorological conditions often do not exceed loss levels for fair weather conditions.

For current loads below critical values, there is an additional differentiation of groups of types of weather conditions: The fifth group is crystalline frost; the sixth group is frost; the seventh group is dew; the eighth group is fog (strong and moderate); the ninth group is rain with an intensity higher than critical; and the tenth group is weather with high air humidity. In general, the recommendations given in [10], in some cases, do not correspond to experimental data for multi-split wires of high-voltage transmission lines, do not take into account many factors affecting the corona, and therefore require further improvement. As for the typical dependences of corona power losses on voltage levels obtained by [20], it is obvious that the use of typical characteristics can lead to significant errors in the calculation and optimization of stationary modes of EPS. In industrial programs for the optimization of EPS modes, as a rule, changes in the values of the parameters of the power transmission line, caused by the influence of meteorological conditions and the load current of the line, are not taken into account.

Changes in parameters are also influenced by other factors: Contamination of wires, corrosion, etc., the influence of which is also not taken into account. Thus, the obtained experimental dependences  $\Delta P_k = f(U)$  are oriented to use only for four main groups of weather conditions. For other groups of weather conditions, the corona power losses are not directly determined, which leads to a distortion of the magnitude of these losses. In existing programs for the optimization of modes, nonlinear dependences  $\Delta P_k = f(U)$  are represented by polynomials of fixed degrees of the form:

$$\Delta P = \left[ a_0 + a_1 \left( \frac{U_p}{U_H} \right) + a_2 \left( \frac{U_p}{U_H} \right)^2 + \dots + a_k \left( \frac{U_p}{U_H} \right)^k \right] l, \quad (15)$$

where  $U_p$  and  $U_H$  are real and nominal nodal voltages, respectively, and  $l$  is the line length. The nonlinear dependences  $\Delta P_k = f(U)$  are represented by the equation of a parabola of the second order. Studies have shown that the approximation of the above curves by a polynomial of a certain fixed degree, in particular by a quadratic polynomial, is not justified. Higher-degree polynomials can lead to greater accuracy. In the general case, it is advisable to have a criterion for determining the optimal degree of the approximating polynomial for these curves.

Therefore, given the fact that meteorological conditions are very diverse—fog, rain with different intensities, dry and wet snow—and the weather in certain sections of the line may be different, to improve the accuracy of optimization of the EPS and regime, it is advisable to promptly determine the characteristics  $\Delta P_k = f(U)$ . The real possibility of obtaining such characteristics is primarily due to the emergence of modern information recorders. In turn, the prompt determination of the dependences of the corona power losses on the voltage presupposes the choice of an effective method for approximating the dependence  $\Delta P_c = f(U)$  and an approach to the correct estimation of the optimal degree of the approximating polynomial.

The methods considered in this work for determining the real dependences of power losses on the corona on the voltage in high-voltage AC transmission lines make it possible to perform operational correction of the dependences  $\Delta P_c = f(U)$  in the EPS models on stationary segments. Thus, as a result of optimization, the values of voltage levels are more accurately calculated at which the total losses of active power (load and corona) are minimal. Due to the fact that the structure of the regression equation is not known in advance, during the calculations using the developed programs, structural-parametric identification was carried out, i.e., selection of the optimal degree of the regression equation and calculation of its coefficients.

Prompt determination of the real dependences of active power losses to the corona on voltage ( $P_c = f(U)$ ) involves two methods of obtaining the necessary initial data—in specially planned modes (no-load, load, line voltage changes by changing the position of transformer transformers in the entire control range) and during operation.

Regardless of the method used to obtain the voltage dependences of the corona power losses, the task is to select an effective approximation method on the stationarity intervals of these real dependences and to determine the statistically substantiated degree of the polynomial. For this purpose, in this work, we carried out comparative studies of three approximation methods [22]: Polynomial regression, sequential regression, and orthogonal Chebyshev polynomials. For the first, the parabolic regression method of the following form was considered:

$$\Delta P_c = a_0 + a_1 U + a_2 U^2 + a_3 U^3 + \dots + a_c U^c \quad (16)$$

Based on the materials available in bulk electrical power systems (curves of the dependence of specific corona losses on voltage, obtained via corresponding measurements of the 750 kV transmission line Vinnitsya-Zapadno-Ukrainskaya for four types of weather), a comparative assessment of the above approximation methods was conducted.

The dependences of the corona power losses on voltage were also calculated for two mixed types of weather conditions for the network model. Since in complex closed networks it is not possible to obtain these characteristics in the same voltage range as in the test spans, the indicated dependences for mixed weather types were obtained in the voltage range determined by the control capabilities of transformer caps. The nature of the dependences of the corona power losses for mixed types of weather conditions differs significantly from the typical characteristics.

Common among the three mentioned approximation methods are two evaluation criteria. The first is the criterion for evaluating the parameters of a mathematical model (least-squares method):

$$F(a) = \sum_{i=1}^n [y_i - f(a, x_i)]^2 \quad (17)$$

where  $x$ , and  $y$  are inputs and output parameters and  $i$ , and  $n$  are the current index and amount of data in the sample, respectively.

The second is the criterion for evaluating the maximum degree of the regression equation  $f(a, x_i)$ :

$$D_k = \frac{1}{n - k - 1} \sum (y_i - a_0 - a_1 x_1 - \dots - a_k x_i^k)^2, \quad (18)$$

where  $D_k$  is the value of the variances between the degree of  $k$  values of the parameters specified and calculated by the regression equation, and  $k$  is the degree of the approximating polynomial. After  $D_{k+1}$  ceases to differ significantly from its previous value  $D_k$ , the increase in the degree  $k$  of the regression equation should be stopped.

The significance of the difference between the values of  $D_k$  and  $D_{k+1}$  is checked by the Fisher test. The compared methods differ from each other in the way that they form the regression equation  $f(a, x_i)$ . To carry out calculations and studies, the corresponding programs for the implementation of these methods were developed.

The programs automatically calculated the coefficients of the approximating polynomials, as well as statistical characteristics: Mathematical expectation, standard deviation, variance, mean deviations, points of maximum and minimum outliers, asymmetry, and kurtosis. The obtained sample distribution was checked for consistency with the normal distribution law.

The efficiency of the developed programs and the reliability of the results were checked for compliance with the results of reference calculations obtained in standard approximation programs. Comparative analysis of the results of reference calculations showed their complete identity.

### 7. Method of Approximation of the Dependences of Power Losses on the Crown on Voltage by the Method of Polynomial Regression

Let us represent the regression equation in matrix form:

$$D_k = \frac{1}{n-k-1} \sum (y_i - a_0 - a_1x_1 - \dots - a_kx_i^k)^2, \quad (19)$$

$$Y = X\alpha + \varepsilon, \quad (20)$$

where  $Y$  is a vector of output parameters;  $X$  is a matrix of independent variables;  $\alpha$  is a vector of unknown estimated parameters; and  $\varepsilon$  is the vector of errors.

The sum of the squares of the errors can be written as:

$$\varepsilon\varepsilon' = (y - x\alpha)^T (y - x\alpha) = y^T y - 2\alpha^T x^T y + \alpha^T x^T x \alpha. \quad (21)$$

Differentiating Equation (18) with respect to the coefficient  $\alpha$  and equating the resulting matrix equation to zero, we obtain a system of normal equations:

$$(x^T x)\hat{\alpha} = x^T y. \quad (22)$$

As a result of solving Equation (19), we obtain the estimated values of the coefficients:

$$\hat{\alpha} = (x^T x)^{-1} x^T y. \quad (23)$$

The method assumes preliminary centering of samples of input and output parameters. In this case, the free term  $a_0$  disappears from the nonlinear Equation (15). To facilitate identification, we introduce new variables  $z$  and write Equation (18) in the linear form:

$$\Delta P = a_1 z_1 + a_2 z_2 + a_3 z_3 + \dots a_k z_k. \quad (24)$$

Let us represent Equation (24) in the matrix form:

$$\Delta P = a^T z. \quad (25)$$

Analogous to Equation (15), the expression for the objective function can be written as follows:

$$F(a) = \sum_{i=1}^n (\Delta P_n - \hat{a}_n^T z_n)^2. \quad (26)$$

Differentiating Equation (26) with respect to an and equating the derivative to zero (to find the minimum of the function  $F(a)$ ), we can obtain the following equality:

$$\left( \sum_{i=1}^n z_i z_i^T \right) \hat{a}_n = \sum_{i=1}^n \Delta P z_i. \quad (27)$$

Introducing the notation:

$$P_n^{-1} = \sum_{i=1}^n (z_i z_i^T) \quad (28)$$

We obtain an expression for estimating the coefficients of the desired regression equation:

$$\hat{a}_n = P_n \sum_{i=1}^n \Delta P_i z_i. \tag{29}$$

After carrying out the appropriate transformations, we obtain Equation (29) in the recurrent form:

$$\hat{a}_n = \hat{a}_{n-1} + P_n z_n (\Delta P_n - z_n^T \hat{a}_{n-1}). \tag{30}$$

In a similar way, one can obtain recurrence relations for the parameter  $P_n$ :

$$P_n = P_{n-1} - P_{n-1} z_n (1 + z_n^T P_{n-1} z_n)^{-1} z_n^T P_{n-1}. \tag{31}$$

Since the expression in parentheses is scalar, there is no need to use the matrix inversion operation. This suggests that, compared to the previously described polynomial regression method, the sequential method has greater computational stability. A feature of this method is the ability to calculate the coefficients of the regression equation by obtaining the first values of the input and output parameters. At each step of obtaining new data, the coefficients are refined up to a change in the stationary segment. At the new stationary interval, the process of calculating and adjusting the regression coefficients is resumed.

In the case of curve approximation using orthogonal Chebyshev polynomials, the approximating polynomial is sought in the form of a sum of polynomials of increasing degrees, and the addition of new terms does not change the coefficients at the previous ones. Successively adding term by term in this way, it is possible to estimate how the sum of the squares of the deviations calculated from the given values decreases.

The general view of the regression equation of the  $k$ th order is:

$$y = a_0 P_0(x) + a_1 P_1(x) + \dots + a_k P_k(x) \tag{32}$$

The coefficients  $a_0, a_1, \dots, a_k$  are also found using the least-squares method by the following formulas:

$$a_0 = \frac{\sum \Delta P_i}{n}, a_1 = \frac{\sum \Delta P_i P_i(U_i)}{\sum P_i^2(U_i)}, \dots, a_k = \frac{\sum \Delta P_i P_k(U_i)}{\sum P_k^2(U_i)}. \tag{33}$$

The polynomials  $P_c(U_i)$  are Chebyshev polynomials. The first of them is:

$$P_0(U) = 1, P_1(U) = U - \frac{n+1}{2}. \tag{34}$$

and the second

$$P_{k+1}(U) = P_1(U)P_k(U) - \frac{k^2(n^2 - k^2)}{4(4k^2 - 1)} P_{k-1}(U). \tag{35}$$

The rest are determined by the formula:

$$D_k = \frac{S_k}{n - k - 1}, \tag{36}$$

where  $S_k$  is sequentially calculated using the following recursive formula:

$$S_k = S_{k-1} - a_k^2 \sum P_k^2(U_i). \tag{37}$$

In turn, the initial value of  $S_0$  is determined as follows:

$$S_0 = \sum [\Delta P_i - a_0 P_0(U)]^2 = \sum (\Delta P_i - \bar{\Delta P})^2 = \sum \Delta P_i^2 - \frac{(\sum \Delta P_i)^2}{n}. \tag{38}$$

When developing an approximation algorithm to the Chebyshev method, the methodology given in [18] was taken as a basis. In the method under consideration, an increase in the approximation accuracy is achieved by complementing the  $k$ th degree polynomial (35) with terms of the form  $a_{k+1} P_{k+1}(x)$ . The coefficients  $a_{k+1}$  and the polynomials  $P_{k+1}(x)$  are calculated using the corresponding formulas. Further transformations are carried out and the polynomial (38) is reduced to the form:

$$y = a_0^{(k+1)} + a_1^{(k+1)}x + a_2^{(k+1)}x^2 + \dots + a_k^{(k+1)}x^k + a_{k+1}^{(k+1)}x^{(k+1)} \quad (39)$$

With this calculation procedure, the reduction of the polynomial to the form (35) is performed every time from (39) after obtaining the next term  $a_k + 1P_{k+1}(x)$ , which is associated with cumbersome algebraic transformations. Therefore, to improve the efficiency of the approximation algorithm by the Chebyshev method, this technique was changed in such a way that the approximating polynomial is directly sought in the form (45), and, to obtain the coefficients  $a_0^{(k+1)}, \dots, a_k^{(k+1)}$  of the polynomial  $(k+1)$  degree, the previously found coefficients of the  $k$ th degree polynomial  $a_0^{(k)}, \dots, a_k^{(k)}$  are used, to which the corrections  $\Delta a_0^{(k+1)}, \dots, \Delta a_k^{(k+1)}$  are conducted:

$$a_0^{(k+1)} = a_0^{(k)} + \Delta a_0^{(k+1)} \quad (40)$$

$$a_k^{(k+1)} = a_k^{(k)} + \Delta a_k^{(k+1)}. \quad (41)$$

Thus, calculations for determining polynomials of the second and subsequent degrees are performed using recursive formulas. In the developed algorithm, to reduce computational errors, not the initial dependence  $y_f = f(x_i)$ , but rather its scaled value  $y_{fM} = f(x_{iM})$  is approximated directly:

$$x_{iM} = \frac{x_{fi}}{x_s}, \quad (42)$$

$$y_{iM} = \frac{y_{fi}}{y_s}, \quad (43)$$

where  $x_s = \frac{1}{n} \sum_{i=1}^n x_{fi}$ ,  $y_s = \frac{1}{n} \sum_{i=1}^n y_{fi}$ .

The scaled values are used to calculate the coefficients of the approximating polynomial:

$$y = a_{0M}^{(k+1)} + a_{1M}^{(k+1)}x + a_{2M}^{(k+1)}x^2 + \dots + a_{kM}^{(k+1)}x^k + a_{(k+1)M}^{(k+1)}x^{(k+1)}, \quad (44)$$

The restoration of the true values of the coefficients of the polynomial (35) is carried out by the formula:

$$a_i = a_{iM} \frac{y_s}{x_s^i} \quad (45)$$

The calculation results using the above method and the same initial data are presented. The initial data for determining the dependence  $\Delta P_k = f(U)$  of four types of weather conditions, obtained as a result of experiments carried out on real power transmission lines of 750 kV, were pre-processed and approximated by these dependences using regression equations carried out in the interpolation area; therefore, the application of the least-squares method based on the "internal" criterion (mean square error at all points) for finding the model of optimal complexity is admissible.

One of the measures that ensure the reduction of electricity losses is the optimization of the modes of electrical networks of power systems in terms of voltage and reactive power. This measure is not associated with large additional costs and can be carried out at the stage of short-term planning and operational management of power systems modes. The question of the expediency of optimizing the overhead line mode by voltage, taking into account corona losses and losses for heating wires, was raised earlier. At this stage of research, the operation of isolated overhead lines was analyzed. The dependences of the

total losses in the line as a function of voltage were considered. By minimizing these losses on individual overhead lines, the optimal operating voltage was found for various weather conditions on the route.

The principal expediency of taking into account corona losses and heating of overhead line wires during voltage regulation was shown. At the same time, the problem of finding the optimal voltage on one of the overhead lines included in the branched system is obviously not equivalent to the problem of optimizing the steady-state modes of the entire network as a whole due to the significant mutual influence of some network sections on others. At the same time, it is necessary to note the variety of operating characteristics of the system elements, the mutual shunting effect of networks of different voltage classes, constantly changing meteorological conditions in individual regions of a large interconnected electrical system (IES), the significant influence of these meteorological conditions on the level of corona power losses on overhead lines, etc.

### 8. Determination of the Dependence $\Delta P_c = F(U)$ on Operationally Determined Values of Active Power Losses per Corona for Use in Optimizing the Modes for Voltage and Reactive Power

As noted, the efficiency of operative optimization of EPS modes in terms of voltage and reactive power will increase when real, operatively determined dependences of active power losses on the corona on nodal voltages at the ends of high-voltage lines ( $\Delta P_k = f(U)$ ) are used in calculations. By continuously monitoring the active power losses per corona during operation, it is possible to check the compliance of the existing standard dependence with the actual operating conditions before performing the optimization.  $\Delta P_1(0)$ ,  $\Delta P_2(0)$ ,  $\Delta P_3(0)$  are used for a narrow range of voltage changes ( $U_1, U_2, U_3$ ). The problem is to restore the dependence curve  $\Delta P(0) = f(0)$ . For the given voltage values ( $U_1, U_2, U_3$ ), we determine the corona losses for four types of weather [15]:

- (1)  $\Delta P_{c1}^{(f)}$ ,  $\Delta P_{K2}^{(f)}$ , and  $\Delta P_{K3}^{(f)}$  are for frost.
- (2)  $\Delta P_{c1}^{(s)}$ ,  $\Delta P_{K2}^{(s)}$ , and  $\Delta P_{K3}^{(s)}$  are for snow.
- (3)  $\Delta P_{c1}^{(r)}$ ,  $\Delta P_{c2}^{(r)}$ , and  $\Delta P_{c3}^{(r)}$  are for rain.
- (4)  $\Delta P_{c1}^{(g)}$ ,  $\Delta P_{c2}^{(g)}$ , and  $\Delta P_{c3}^{(g)}$  are for good weather.

We determine the differences between the operatively determined values of corona losses  $\Delta P(0)$  and the value of  $\Delta P_c$  for four types of weather for the same stress values:

- (a)  $\Delta P_c(0) - \Delta P_c^{(f)} = \delta P_c^{(0-f)}$ ,
- (b)  $\Delta P_c(0) - \Delta P_c^{(s)} = \delta P_c^{(0-s)}$ ,
- (c)  $\Delta P_c(0) - \Delta P_c^{(r)} = \delta P_c^{(0-r)}$ ,
- (d)  $\Delta P_c(0) - \Delta P_c^{(g)} = \delta P_c^{(0-g)}$ .

By the signs of these differences, one can judge which typical curves should lie between the operatively determined dependence  $\Delta P_c^{(0)} = f^{(0)}(U)$ . Consider the following options.

In the case that the operationally determined values of losses coincide or are close to one of the typical curves, then this typical curve can be used.

If the operationally determined values of losses do not correspond to any of the typical dependences, we can proceed as follows—either reconstruct the new dependence  $\Delta P_c^{(0)} = f^{(0)}(U)$ , conducting an active experiment, or use the nearest typical dependence and construct a similar one.

Consider the first, which is more complex to implement from an operational point of view. To construct the real dependence  $\Delta P_c^{(0)} = f^{(0)}(U)$  by conducting an active experiment, it is necessary to change the voltage within the allowable limits by calculating the autotransformer and taps and to calculate the power loss per corona at these values. The structural-parametric identification of the obtained dependence  $\Delta P_c = f(U)$  can then be performed using orthogonal Chebyshev polynomials, and Fisher's criterion can be used to estimate the required degree of the approximating polynomial. Thus, when optimizing the current modes in terms of voltage and reactive power, the operationally determined dependence  $\Delta P_c^{(0)} = f^{(0)}(U)$  corresponding to the real conditions will be used.

Consider the second approach, namely the construction of the dependence  $\Delta P_c^{(0)} = f^{(0)}(U)$  by analogy with the nearest typical curve.

Assume that  $\delta P_c^{(0-i)}$  and  $\delta P_c^{(0-d)}$  are negative, and  $\delta P_c^{(0-s)}$  and  $\delta P_c^{(0-g)}$  are positive, then the operatively determined curve  $\Delta P_c^{(0)} = f^{(0)}(U)$  should lie between typical curves for snow and rain. It is necessary to determine the values of corona losses  $\Delta P_c^{(0)} = f^{(0)}(U)$  outside the range of measured stresses and corona losses determined by them.

To do this, we proceed as follows: Supposing  $U_1 < U_2 < U_3$ , we compare the absolute values of the differences  $\delta P_{c(0-s)}$  and  $\delta P_{c(0-d)}$ , assume that  $|\delta P_{c(0-s)}| > |\delta P_{c(0-d)}|$ , then the operatively determined  $\Delta P_c^{(0)} = f_0(U)$  lies closer to the typical curve for rain and is similar in shape.

The required values of  $\Delta P_c^{(0)}$  are determined as follows: For all values of stresses  $U_i < U_1$ , we determine the values of corona losses for rain  $\Delta P_{ci}$ . Moreover,  $\Delta P_{ci} > \Delta P_{ci-1} > \Delta P_{ci-2}$ . We do the same for the values of stresses  $U_i > U_3$ ,  $\Delta P_{ci} < \Delta P_{ci+1} < \Delta P_{ci+2}$ .

Now, from all  $i$ -th values of  $\Delta P_{ci}$ , we subtract the values of  $\delta P_c^{(0-d)}(U_1)$  found at the voltage  $U_1$ , and from all points  $i$ , we subtract the values of  $\delta P_c^{(0-d)}(U_3)$  found at the point  $U_3$ .

From all operatively found values of corona losses  $\Delta P_{c1}$ ,  $\Delta P_{c2}$ ,  $\Delta P_{c3}$  and restructured values of  $\Delta P_{ci}$  and  $\Delta P_{cl}$  we determine the regression dependence  $\Delta P_c^{(0)} = f^0(U)$ , which can be further used in optimizing the voltage and reactive mode power.

## 9. Future Directions

Further research will aim to analyze the possibility of using low-phase modes to increase the efficiency of main electrical networks. The values of asymmetry coefficients in the application of incomplete-phase modes of operation of autotransformers and shunt reactors will be determined in order to develop technical means of compensation of incomplete-phase modes. To confirm the effectiveness of the proposed tools, comparative calculations will be performed by conducting simulations.

A theoretical approach and analytical expressions will also be proposed, which will allow one to determine the currents and voltages of the phase windings of the autotransformer in arbitrary asymmetric modes of operation, using the factory characteristics of the equipment and the current parameters of the modes. When using existing mathematical models and the results of calculation of incomplete phase modes, it must be remembered that the traditional method of symmetric components is based on the assumption of constancy of parameters of the substitution scheme, and the accuracy of the calculation of certain asymmetric modes is low. In particular, research should assess the modules and angles of the vectors of currents and voltages in the windings of a three-phase autotransformer in one of the characteristic asymmetric modes at break of one of the voltage phases and its simultaneous short circuit to the ground by the autotransformer, taking into account the electromagnetic connection of the windings. Based on these data, vector diagrams will be constructed, which give a clear idea of the peculiarities of such modes.

## 10. Technical Means of Suppression of Resonance Phenomena in Electrical Networks

At present, more and more attention is being paid to FACTS technology, since it is obvious that the construction of additional parallel lines to increase the throughput of individual sections of the EPS is economically ineffective and also entails additional problems associated with the alienation of large plots of land for the line route, the complication of switchgear at substations, increased voltage values along the line length in modes close to no-load, etc. [23,24].

Based on the operating modes of EHV, the power flow through them changes significantly both during the day and seasonally. In addition, given the development industries of countries, as well as an increase in the number of energy-intensive household devices that require more and more electricity, there is a need to increase the transmission capacity of EHV. The desire to increase the throughput leads to the need to grant the lines the properties of controllable or flexible lines changing the parameters in the function of the EPS operation

mode [25,26]. Thus, power transmission data from passive elements are converted into active ones and affect the EPS operation modes. It covers both power transmission lines as a whole and individual devices participating in the control of the operating modes of electrical networks (ENs) [27].

Figure 5a,b shows EHV with installed controlled shunt reactors.

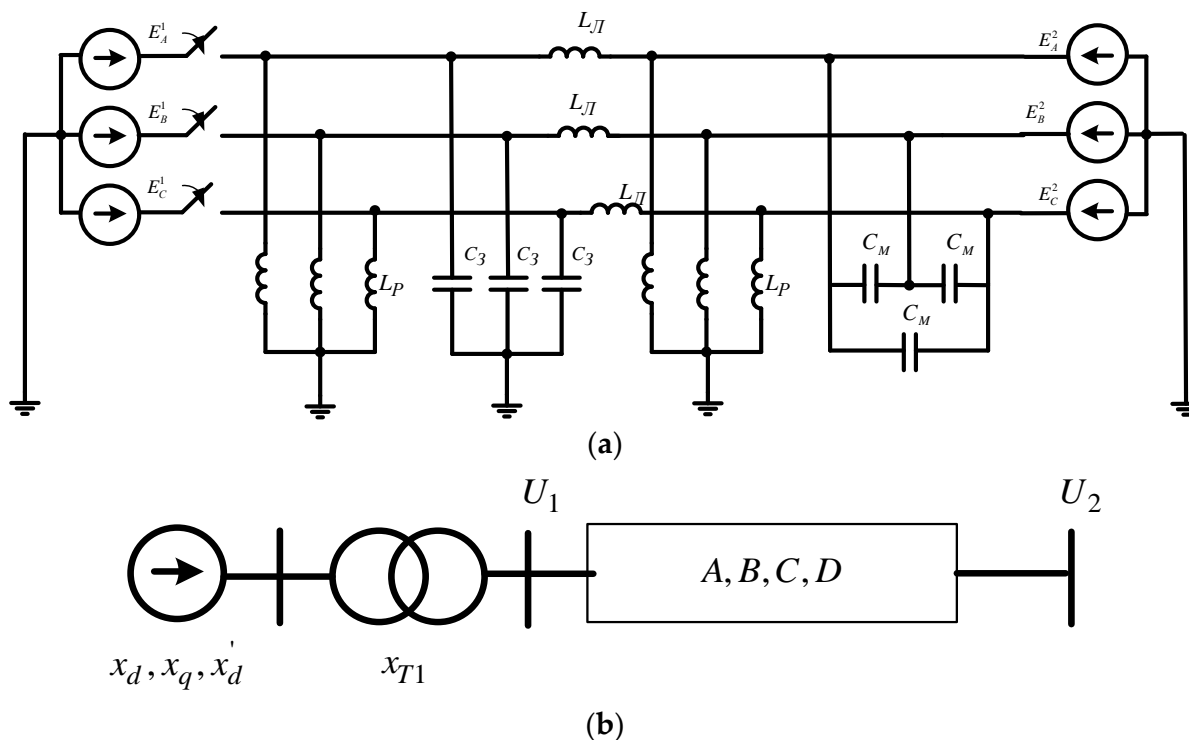


**Figure 5.** Schematic representation of a line with installed controlled shunt reactors: (a) is equivalent circuit of an extra-high voltage transmission line with an uncontrolled shunt reactor and (b) is schematic representation of a power line with generator values along the longitudinal and transverse axes.

In the case of the installation of CSR, it is possible to control the degree of compensation of charging power so as to deviate from a zone of self-excitation of generators. This is possible due to the fact that CSR is able to work with normalized overload up to 130% and short-term overload up to 200%. In this case, the charging power can be compensated for in such a way that the synchronous generator will not work with a capacitive load.

The main feature of the modes of long-distance power transmission lines with compensated reactance is the need to maintain an optimal ratio between the voltages across power transmission lines due to the high sensitivity of efficiency and reactive power to this ratio. The relationship between the conditions for regulating CSR and the regime parameters of power transmission is determined. The idealized CSR control equation was taken in the form:

$$\Delta b_{CSR}^{(i)}(1 + pT_{CSR}^{(i)}) = k_{0U}^{(i)}\Delta U_i \tag{46}$$

where  $b_{CSR}^{(i)}$  is admittance CSR in the  $i$ -th node;  $T_{CSR}^{(i)}$  is the reactor time constant;  $k_{0U}^{(i)} \left[ \frac{\text{units conductivity}}{\text{units voltage}} \right]$  is the coefficient of regulation of the conductivity of the reactor by voltage deviation,

$$\Delta U_i = U_i - U_{i(0)}, \Delta b_{CSR}^{(i)} = b_{CSR}^{(i)} - b_{CSR0}^{(i)} \tag{47}$$



It is shown that the conductivity of the reactor, at given voltages at  $(i - 1), i, (i + 1)$  nodes, is:

$$b_{CSR}^{(i)} = \frac{U_{(i-1)}}{U_i B_i} \cos \delta_{(i-1)i} + \frac{U_{(i+1)}}{U_i B_2} \cos \delta_{(i+1)i} - \frac{A_1}{B_1} - \frac{D_2}{B_2} \tag{48}$$

where  $A_1, B_1, C_1, D_1, A_2, B_2, C_2, D_2$  are parameters of the sections of the line with constant voltage at the ends adjacent to the node for connecting the reactors.

From the analysis of expressions (47) and (48), it can be seen that the coefficient  $k_{0U}^{(i)}$ , regarding the regulation of CSR required to maintain the stresses in the  $i$ -th node with a given accuracy, is determined only by the parameters of the sections adjacent to the reactor connection node and does not depend on the geometric the length of the line as a whole.

The analysis of expressions (47) and (48) shows that the coefficient of regulation of CSR required to maintain voltages in the  $i$ -th node with a given accuracy is determined only by the parameters of the section adjacent to the reactor connection node and does not depend on the line length. Analytical expressions for the coefficients of the characteristic polynomial are obtained after expanding the power of the operator “ $p$ ” determinant of the system of equations of small perturbations (ignoring the transients in the stator circuits) in the absence of excitation control and neglect of the damping circuits of generators. Figure 6 shows zone 1 of synchronous self-excitation and zones 2 and 3 of asynchronous self-excitation.

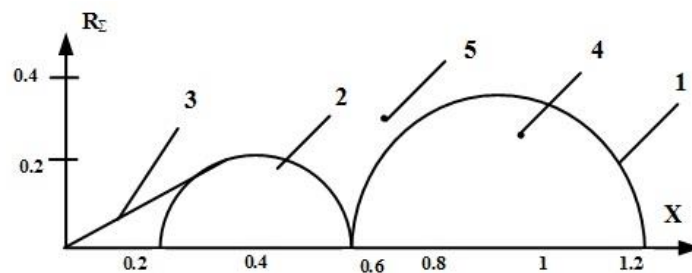


Figure 6. Zone 1 of synchronous self-excitation and zones 2 and 3 of asynchronous self-excitation.

To exclude these rather large zones, it is necessary to reduce the effect of the transverse damping circuit, i.e., the time constant of this circuit must be either very small or large enough. It is impossible to completely eliminate the transverse damping circuit under the conditions of self-unloading of the generator in low load modes. Increasing the active resistance of the line in order to suppress self-excitation is ineffective, as it leads to a decrease in efficiency and power transmission.

Therefore, for the maximum increase in a zone of steady work, the following measures are necessary:

- Selection of parameters of damping contours providing the maximum reduction of a zone of asynchronous self-excitation;
- Increase in the transient resistance of the generator;
- An increase in reactive resistances of final transformers.

In order to analyze the effectiveness of controlled shunt reactors, the effect of changes in the inductance of CSR on the total inductive resistance was evaluated (48).

In order to prevent the self-excitation of generators, the point with coordinates  $X_\Sigma$  and  $R_\Sigma$  should be outside the areas of self-excitation. Coordinates are determined by the following formulas:

$$X_\Sigma = \frac{Z_W(X_1 + X_{CSR})(X_{CSR1} + X_{CSR2}) \cos \lambda + (Z_W^2(X_1 + X_{CSR1}) - X_{CSR1}X_1X_{CSR2}) \sin \lambda}{(X_{CSR1}X_{CSR2} - Z_W^2) \sin \lambda - Z_W(X_{CSR} + X_{CSR2}) \cos \lambda} \tag{49}$$

$Z_W$  is the line impedance and  $X_{CSR}$  is the equivalent resistance of two CSR groups.  $X_{CSR1}$ ,  $X_{CSR2}$  are the resistance of the first and second groups of CSR, respectively, while  $\lambda$  is the wavelength of the line. Values for the scheme in Figure 5b are found by the formula:

$$R_{\Sigma} = R + R_T + R_G \quad (50)$$

To analyze the self-excitation of generators, calculations were performed for the ultra-high-voltage power transmission line with the following values:  $l = 300$  km is the line length,  $U = 750$  kV is the nominal line voltage, a wire phase design 4xASO-400/93, characterized by the following parameters  $r_0 = 0.019$  Ohm/km;  $x_0 = 0.289$  Ohm/km;  $g_0 = 0.0325$   $\mu$ S/km;  $b_0 = 4.13$   $\mu$ S/km.

The results of calculations when installing uncontrolled shunt reactors in the electrical network are shown in Figure 6, with point number 4. Point number 4 falls into the zone of synchronous self-excitation.

## 11. Discussion and Comparing the Performance/Implication of the Presented Methods

On the basis of the data available at the National Power Company “Ukrenergo”, built curves of the specific corona losses depend on the voltage. The obtained results of appropriate measurements of the 750 kV power transmission line Vinnytsya-Zapadno-Ukrainskaya for four types of weather are shown in Table 1 and Figure 7.

**Table 1.** Specific active power losses per corona at various voltage values on the 750 kV power transmission line Vinnitsa-Zapadno-Ukrainskaya for typical weather conditions.

№	Voltage, [MW]	Specific Active Power Losses per Corona, [MW/km]			
		Good Weather	Dry Snow	Rain	Frost
1	0.67	0.00320	0.01080	0.03960	0.11700
2	0.68	0.00340	0.01200	0.04300	0.12500
3	0.69	0.00380	0.01350	0.04700	0.13500
4	0.70	0.00420	0.01500	0.05120	0.14600
5	0.71	0.00455	0.01635	0.05600	0.15600
6	0.72	0.00510	0.01820	0.06005	0.16700
7	0.73	0.00575	0.02000	0.06500	0.17800
8	0.74	0.00640	0.02240	0.07000	0.18900
9	0.75	0.00710	0.02480	0.07500	0.20200
10	0.76	0.00785	0.02760	0.08080	0.21400
11	0.77	0.00880	0.03050	0.08600	0.22600
12	0.78	0.00980	0.03370	0.09180	0.23800
13	0.79	0.01100	0.03710	0.09700	0.25200
14	0.80	0.01230	0.04135	0.10300	0.26500
15	0.81	0.01380	0.04560	0.10860	0.27800
16	0.82	0.01555	0.05135	0.11400	0.29200
17	0.83	0.01750	0.05500	0.12050	0.30400

Since in complex closed networks it is not possible to obtain these characteristics in the same voltage range as in experimental spans, in this paper, we proposed using these dependencies for mixed types of weather obtained in the voltage range, determined by the control characteristics of the transformers.

The results of calculations based on the above algorithm and the initial data of Table 1 are shown in Table 2. In Table 2, the results of approximation and the obtained coefficient of polynomials are presented.

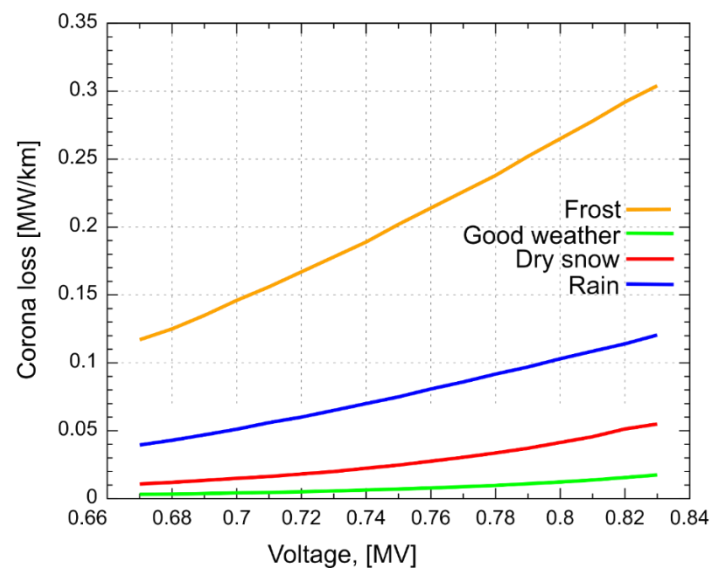


**Figure 7.** Dependences of the specific losses of active power per corona on the voltage at the 750 kV power transmission line Vinnitsa-Zapadno-Ukrainskaya for typical weather conditions (National Power Company “Ukrenergo”).

**Table 2.** Results of approximation and obtained coefficient of polynomials.

Weather Type	Degree	Polynomial Coefficients					Dispersion $D_k$	$D_k/D_{k+1}$
		$a_0$	$a_1$	$a_2$	$a_3$	$a_4$		
Frost	1	-0.684	1.185				$1.08 \times 10^{-5}$	21.12
	2	0.1078	0.935	1.414			$0.51 \times 10^{-5}$	1.77
	3	2.1774	-9.256	12.54	-4.94		$2.89 \times 10^{-7}$	0.97
	4	0.6268	-0.936	-0.418	9.95	-4.968	$3.19 \times 10^{-7}$	0.58
	5	-21.567	100.8	-151.2	38.96	87.22	-54.22	$5.33 \times 10^{-7}$
Rain	1	-0.3063	0.511				$2.847 \times 10^{-6}$	19.29
	2	0.0985	-0.573	0.723			$1.47 \times 10^{-7}$	0.67
	3	0.1401	-5.808	7.720	-3.11		$0.55 \times 10^{-7}$	0.93
	4	1.6588	-7.194	10.51	-5.591	0.828	$0.59 \times 10^{-7}$	0.35
	5	16.811	-76.75	111.0	-25.43	-62.20	37.07	$1.66 \times 10^{-7}$
Dry snow	1	-0.1759	0.272				$9.158 \times 10^{-6}$	40.53
	2	0.5611	-1.702	1.316			$0.226 \times 10^{-6}$	2.13
	3	-0.9362	4.318	-6.731	3.576		$0.106 \times 10^{-6}$	0.94
	4	-1.957	9.798	-17.74	13.39	-3.272	$0.113 \times 10^{-6}$	0.21
	5	-33.995	156.9	-230.2	55.32	130.0	-78.38	$0.565 \times 10^{-6}$
Good weather	1	-0.0556	0.085				$1.368 \times 10^{-6}$	29.11
	2	0.2279	-0.674	0.506			$0.47 \times 10^{-7}$	9.4
	3	-0.6386	2.81	-4.151	2.07		$0.5 \times 10^{-8}$	0.6
	4	0.3255	-2.364	6.242	-7.191	3.089	$0.3 \times 10^{-8}$	0.33
	5	16.431	-76.29	113.1	-28.27	-63.9	39.40	$1.1 \times 10^{-8}$

## 12. Conclusions

The efficiency of operational optimization of EPS modes in terms of voltage and reactive power will increase when the calculations employ real, or close to real, dependences of active power losses per corona from the nodal voltages at the ends of high-voltage lines.

The conducted studies have shown that the approximation of the dependences of the active power losses to the corona on the voltage by a polynomial of one fixed degree (in particular, the second) for various weather conditions is not justified. The use of polynomials of higher degrees leads to greater accuracy of calculations. In a general case, it is necessary to use the criterion for determining the minimum required degree of the approximating polynomial, depending on the specific weather conditions and the voltage level on the EHV.

It is advisable to approximate the dependences of active power losses in the corona on the voltage using orthogonal Chebyshev polynomials, and to estimate the minimum required degree of the approximating polynomial, using the Fisher criterion.

For the first time, on the basis of the operatively determined active power losses to the corona, a method is proposed for the operative determination of the dependence of corona losses on the voltage, which makes it possible to increase the accuracy of the operative optimization of the electric power system modes. It is substantiated that for the approximation of this dependence, it is most expedient to use the Chebyshev orthogonal polynomials, and to determine the minimum required degree of the polynomial one should use the Fisher's statistical criterion.

The article analyzes the self-excitation of a synchronous generator during the restoration of the power system caused by the capacitive load. The use of CSR on the lines allows eliminating the cause of self-excitation of the synchronous generator without the use of special additional measures. The paper substantiates the use of CSR in the derivation of a synchronous generator from the self-excitation mode due to the simultaneous application of the approach of zone determination and determination of a point with coordinates and  $R_{\Sigma}$ .

Synchronous self-excitation is inherent to only explicit-pole generators, with either closed or open excitation winding. Asynchronous self-excitation occurs only with closed excitation winding. In salient and asymmetrical implicit machines, it is accompanied by beatings of current and voltage. Synchronous self-excitation conditions show a smooth change of current and voltage to a certain steady-state value determined by the saturation of the machine. Self-excitation develops only when exceeding the residual voltage of the machine by some critical value, which is about 0.2–0.4% of the rated voltage generator. Artificial demagnetization of generators before the line voltage rises or in the process of lifting can be an effective measure to prevent self-excitation and allow one to turn on the machines to the line for self-synchronization. Methods of mathematical modeling, an algorithm, and a program focused on the study of transient modes of long-distance power lines with CSR have been developed.

**Author Contributions:** Conceptualization, V.K., O.R., M.D. and O.M.; methodology, P.V., H.A.A., M.Q., I.T. and S.K.; validation, V.K., S.K., P.V., O.R., O.M. and M.D.; formal analysis, V.K.; investigation, T.S.; resources, V.K., O.R. and O.M.; writing—original draft preparation, V.K., H.A.A., M.Q., I.T., S.K., O.R., T.S. and O.M.; writing—review and editing, V.K., O.R., I.T., O.M. and M.D. All authors have read and agreed to the published version of the manuscript.

**Funding:** This research received no external funding.

**Data Availability Statement:** The data presented in this study are available upon request from the corresponding author.

**Conflicts of Interest:** The authors declare no conflict of interest. The funders had no role in the design of the study; in the collection, analyses, or interpretation of data; in the writing of the manuscript; or in the decision to publish the results.

## References

1. Singh, G.K. Self-Excited Induction Generator Research—A Survey. *Electr. Power Syst. Res.* **2004**, *69*, 107–114. [CrossRef]
2. Grantham, C.; Sutanto, D.; Mismail, B. Steady-state and Transient Analysis of Self-Excited Induction Generators. *IEE Proc. B Electr. Power Appl.* **1989**, *136*, 61–68. [CrossRef]
3. Levi, E.; Sokola, M.; Boglietti, A.; Pastorelli, M. Iron Loss in Rotor-flux-oriented Induction Machines: Identification, Assessment of Detuning and Compensation. *IEEE Trans. Power Electron.* **1996**, *11*, 698–709. [CrossRef]
4. Leidhold, R.; Garcia, G.; Valla, M.I. Field-Oriented Controlled Induction Generator with Loss Minimization. *IEEE Trans. Ind. Electron.* **2002**, *49*, 147–156. [CrossRef]
5. Seyoum, D. The Dynamic Analysis and Control of a Self-Excited Induction Generator Driven by a Wind Turbine. Ph.D. Thesis, School of Electrical Engineering and Telecommunications, UNSW, Sydney, Australia, 2003.
6. Wee, S.D.; Shin, M.H.; Hyun, D.S. Stator-Flux-Oriented Control of Induction Motor Considering Iron Loss. *IEEE Trans. Ind. Electron.* **2001**, *48*, 147–156. [CrossRef]
7. Sandhu, K.S.; Joshi, D. Steady State Analysis of Self-Excited Induction Generator using Phasor-Diagram Based Iterative Model. *WSEAS Trans. Power Syst.* **2008**, *3*, 715–724.
8. Sandhu, K.S.; Joshi, D. A Simple Approach to Estimate the Steady-State Performance of Self-Excited Induction Generator. *WSEAS Trans. Syst. Control* **2008**, *3*, 208–218. [CrossRef]
9. Feltes, J.W.; Grande-Moran, C. Black Start Studies for System Restoration. In Proceedings of the 2008 IEEE Power and Energy Society General Meeting—Conversion and Delivery of Electrical Energy in the 21st Century, Pittsburgh, PA, USA, 20–24 July 2008. [CrossRef]
10. Al-Hamouz, Z.M.; Abdel-Salam, M.; Al-Shehri, A.M. Inception voltage of corona in bipolar ionized fields-effect on corona power loss. *IEEE Trans. Ind. Appl.* **1998**, *34*, 57–65. [CrossRef]
11. Riba, J.R.; Abomailek, C.; Casals-Torrens, P.; Capelli, F. Simplification and cost reduction of visual corona tests. *Gener. Transm. Distrib. IET* **2018**, *12*, 834–841. [CrossRef]
12. Hernandez-Guiteras, J.; Riba, J.R.; Casals-Torrens, P.; Bosch, R. Feasibility analysis of reduced-scale air breakdown tests in high voltage laboratories combined with the use of scaled test cages. *IEEE Trans. Dielectr. Electr. Insul.* **2013**, *20*, 1590–1597. Available online: <https://ieeexplore.ieee.org/document/6633688> (accessed on 7 March 2022). [CrossRef]
13. Lü, F.C.; Geng, Q.Z.; Liu, Y.P. The Design of Simulating Different Altitudes Ionic Mobility Measuring Device. *Appl. Mech. Mater.* **2013**, *157*, 333–335. [CrossRef]
14. Lei, C.; Tian, W. Probability-Based Customizable Modeling and Simulation of Protective Devices in Power Distribution Systems. *Energies* **2022**, *15*, 199. [CrossRef]
15. Khan, A.N.; Imran, K.; Nadeem, M.; Pal, A.; Khattak, A.; Ullah, K.; Younas, M.W.; Younis, M.S. Ensuring Reliable Operation of Electricity Grid by Placement of FACTS Devices for Developing Countries. *Energies* **2021**, *14*, 2283. [CrossRef]
16. Ordóñez, C.A.; Gómez-Expósito, A.; Maza-Ortega, J.M. Series Compensation of Transmission Systems: A Literature Survey. *Energies* **2021**, *14*, 1717. [CrossRef]
17. Relić, F.; Marić, P.; Glavaš, H.; Petrović, I. Influence of FACTS Device Implementation on Performance of Distribution Network with Integrated Renewable Energy Sources. *Energies* **2020**, *13*, 5516. [CrossRef]
18. Khasawneh, A.; Qawaqzeh, M.; Kuchanskyy, V.; Rubanenko, O.; Miroschnyk, O.; Shchur, T.; Drechny, M. Optimal Determination Method of the Transposition Steps of An Extra-High Voltage Power Transmission Line. *Energies* **2021**, *14*, 6791. [CrossRef]
19. Al-Issa, H.A.; Qawaqzeh, M.; Khasawneh, A.; Buinyi, R.; Bezruchko, V.; Miroschnyk, O. Correct Cross-Section of Cable Screen in a Medium Voltage Collector Network with Isolated Neutral of a Wind Power Plant. *Energies* **2021**, *14*, 3026. [CrossRef]
20. Kuchanskyy, V.; Rubanenko, O. Influence assessment of autotransformer remanent flux on resonance overvoltage. *UPB Sci. Bull. Ser. C Electr. Eng.* **2020**, *82*, 233–250. Available online: <https://www.researchgate.net/publication/343425681> (accessed on 7 March 2022).
21. Kuchanskyy, V.; Satyam, P.; Rubanenko, O.; Hunko, I. Measures and technical means for increasing efficiency and reliability of extra high voltage transmission lines. *Prz. Elektrotech.* **2020**, *11*, 135–141. [CrossRef]
22. Ozioko, I.O.; Okoli, C.C.; Ajah, N.G.; Ugwuanyi, N.S. Enhancement of Power System Transmission Using Static Synchronous Compensator (STATCOM). In Proceedings of the 2019 IEEE PES/IAS PowerAfrica, Abuja, Nigeria, 20–23 August 2019; pp. 482–486. [CrossRef]
23. Kuznetsov, V.; Tugay, Y.; Kuchanskyy, V. Influence of corona discharge on the internal overvoltages in highway electrical networks. *Tekhnichna Elektrodyn.* **2017**, *6*, 55–60. [CrossRef]
24. Kumar, P. Application of fact devices for voltage stability in a power system. In Proceedings of the 2015 IEEE 9th International Conference on Intelligent Systems and Control (ISCO), Coimbatore, India, 9–10 January 2015; pp. 1–5. [CrossRef]
25. Blinov, I.V.; Zaitsev, I.O.; Kuchanskyy, V.V.; Babak, V.P.; Isaienko, V.I.; Zaporozhets, A.O. Problems, methods and means of monitoring power losses in overhead transmission lines. In *Systems, Decision and Control in Energy*; Springer: Cham, Switzerland, 2020; Volume 298, pp. 123–136. [CrossRef]
26. Ko, W.-H.; Gu, J.-C. Design and application of a thyristor switched capacitor bank for a high harmonic distortion and fast changing single-phase electric welding machine. *Power Electron. IET* **2016**, *9*, 2751–2759. [CrossRef]
27. Ciešlik, S. Mathematical Modeling of the Dynamics of Linear Electrical Systems with Parallel Calculations. *Energies* **2021**, *14*, 2930. [CrossRef]